

RNASeq analysis of differentiated keratinocytes reveals a massive response to late events during human papillomavirus type 16 infection, including loss of epithelial barrier function.

KLYMENKO, Tetyana, GU, Q., HERBERT, I., STEVENSON, A., ILIEV, V., WATKINS, G., POLLOCK, C., BHATIA, R., CUSCHIERI, K., HERZYK, P., GATHERER, D. and GRAHAM, S.V.

Available from Sheffield Hallam University Research Archive (SHURA) at:

<https://shura.shu.ac.uk/17090/>

This document is the Accepted Version [AM]

Citation:

KLYMENKO, Tetyana, GU, Q., HERBERT, I., STEVENSON, A., ILIEV, V., WATKINS, G., POLLOCK, C., BHATIA, R., CUSCHIERI, K., HERZYK, P., GATHERER, D. and GRAHAM, S.V. (2017). RNASeq analysis of differentiated keratinocytes reveals a massive response to late events during human papillomavirus type 16 infection, including loss of epithelial barrier function. *Journal of Virology*, JVI.01001-17. [Article]

Copyright and re-use policy

See <http://shura.shu.ac.uk/information.html>

1 **RNASeq analysis of differentiated keratinocytes reveals a massive response to late**
2 **events during human papillomavirus type 16 infection, including loss of epithelial**
3 **barrier function.**

4 Klymenko, T.^{1,6}, Gu, Q.¹, Herbert, I.¹, Stevenson, A.¹, Iliev V.¹, Watkins, G¹., Pollock, C¹.,
5 Bhatia R.², Cuschieri, K.^{2,3}, Herzyk, P.⁴, Gatherer, D.⁵ and Graham, S.V.^{1*}

6 ¹ MRC-University of Glasgow Centre for Virus Research; Institute of Infection, Immunity and
7 Inflammation; College of Medical, Veterinary and Life Sciences, University of Glasgow,
8 Garscube Estate, Glasgow, G61 1QH, Scotland, UK.

9 ² HPV Research Group, University of Edinburgh, 49 Little France Crescent, Edinburgh,
10 EH16 4TJ, Scotland, UK.

11 ³ Specialist Virology Centre, Royal Infirmary of Edinburgh, 51 Little France Crescent,
12 Edinburgh. EH16 4SA, Scotland, UK.

13 ⁴ Institute of Molecular Cell and Systems Biology; Glasgow Polyomics; University of
14 Glasgow, Garscube Estate, Glasgow, G61 1QH, Scotland, UK.

15 ⁵Division of Biomedical & Life Sciences, Faculty of Health & Medicine, Lancaster University,
16 Lancaster, LA1 4YW, UK.

17 ⁶Current address: Biosciences and Chemistry Department, Faculty of Health and Wellbeing,
18 Sheffield Hallam University, Sheffield, S1 1WB, UK.

19 ***Corresponding author.**

20 Rm 254, Jarrett Building, Garscube Estate, University of Glasgow, Glasgow, G61 1QH,
21 Scotland, UK.

22 Tel: 44 141 330 6256; Fax: 44 141 330 5602;

23 e-mail: Sheila.Graham@gla.ac.uk

24

25 **Running title:** RNASeq analysis of keratinocyte response to HPV16 infection.

26 **Abstract:** 241 words. **Text:** 5067 words.

27 **Abstract**

28 The human papillomavirus (HPV) replication cycle is tightly linked to epithelial cell
29 differentiation. To examine HPV-associated changes in the keratinocyte transcriptome,
30 RNAs isolated from undifferentiated and differentiated cell populations of normal,
31 spontaneously immortalised, keratinocytes (NIKS), and NIKS stably transfected with HPV16
32 episomal genomes (NIKS16), were compared using RNASeq. HPV16 infection altered
33 expression of 2862 cellular genes. Next, to elucidate the role of keratinocyte gene
34 expression in late events during the viral life cycle, RNASeq was carried out on triplicate
35 differentiated populations of NIKS (uninfected) and NIKS16 (infected). Of the top 966 genes
36 altered ($>\log_2 = 1.8$, 3.5-fold change) 670 genes were downregulated and 296 genes were
37 up-regulated. HPV down-regulated many genes involved in epithelial barrier function that
38 involves structural resistance to the environment and immunity to infectious agents. For
39 example, HPV infection repressed expression of the differentiated keratinocyte-specific
40 pattern recognition receptor TLR7, the Langerhans cell chemoattractant, CCL20, and
41 proinflammatory cytokines, IL1A and IL1B. However, IRF1, IFN κ and viral restriction factors
42 (IFIT1, 2, 3, 5, OASL, CD74, RTP4) were up-regulated. HPV infection abrogated gene
43 expression associated with the physical epithelial barrier, including keratinocyte
44 cytoskeleton, intercellular junctions and cell adhesion. qPCR and western blotting confirmed
45 changes in expression of seven of the most significantly altered mRNAs. Expression of three
46 genes showed statistically significant changes during cervical disease progression in clinical
47 samples. Taken together, the data indicate that HPV infection manipulates the differentiating
48 keratinocyte transcriptome to create an environment conducive to productive viral replication
49 and egress.

50

51 **Importance**

52 Human papillomavirus (HPV) genome amplification and capsid formation takes place in
53 differentiated keratinocytes. The viral life cycle is intimately associated with host cell
54 differentiation. Deep sequencing (RNASeq) of RNA from undifferentiated and differentiated
55 uninfected and HPV16-positive keratinocytes showed that almost 3000 genes were
56 differentially expressed in keratinocyte due to HPV16 infection. Strikingly, the epithelial
57 barrier function of differentiated keratinocytes, comprising keratinocyte immune function and
58 cellular structure, was found to be disrupted. These data provide new insights into virus-host
59 interaction crucial for production of infectious virus and reveal that HPV infection remodels
60 keratinocytes for completion of the virus replication cycle.

61

62

63

64

65 Key words: human papillomavirus type 16, epithelial differentiation, keratinocyte
66 transcriptome, cervical disease.

67

68 **Introduction**

69 Human papillomaviruses (HPVs) infect keratinocytes, causing mainly benign lesions or warts
70 (1). Infection is usually transient and is cleared by the immune system (2). However,
71 persistent infection with “high risk” HPV genotypes (HR-HPV) can cause tumour progression
72 to cervical (3), other anogenital (anal, penile, vulvar and vaginal) (4) and oropharyngeal
73 cancers (5). In the case of the cervix, cervical intraepithelial neoplasia (CIN) generally
74 precedes cervical cancer progression (6). CIN1 is thought to represent a transient HPV
75 infection, while CIN3 represents clinically significant, persistent HPV infection that may, if left
76 untreated, progress to cervical cancer (7).

77 The pathway of epithelial cell differentiation, from basal to granular layer, is tightly controlled
78 by complex patterns of keratinocyte gene expression (8). The HPV infectious life cycle is
79 tightly linked to epithelial differentiation. HPV infects basal epithelial cells where it begins to
80 express its genome. The viral replication factor E1 and its auxiliary protein, E2, which is also
81 the viral transcription factor, together with the regulatory proteins E6 and E7 are expressed
82 early in infection. E2, E6 and E7 have each been shown to control cellular gene expression
83 (6). Viral gene expression required for vegetative viral genome amplification takes place in
84 differentiating keratinocytes in the mid to upper epithelial layers (9). At this stage other viral
85 regulatory proteins E4 and E5 that can regulate the host cell are expressed (6). Finally, L1
86 and L2 capsid protein synthesis and virion formation takes place in granular layer
87 keratinocytes and virions are shed from the surface of the epithelium in dead squames (10).
88 The epithelium presents a barrier to the environment and to infectious agents (11).
89 Differentiated keratinocytes possess a dense filamentous network comprised of keratins and
90 other molecules such as filaggrin. Moreover, keratinocytes have an important role in innate
91 and adaptive immunity, and cytokines, chemokines and other immune signalling molecules
92 released by these cells are essential for epithelial homeostasis (12). HPVs have evolved to
93 modulate the epithelium to allow infection, virion formation and egress (6), and many means
94 by which HPV evades the immune response have been documented (13). Elucidating the

95 interactions between HPV and the infected keratinocyte is key to understanding the HPV life
96 cycle and how persistent infection may facilitate development of cervical disease.

97 A number of previous studies have used a microarray approach to further our understanding
98 of the HPV infectious life cycle and cancer progression. The first compared gene expression
99 in normal keratinocytes with that in HPV31-infected keratinocytes (14). Two subsequent
100 studies examined gene expression changes during tumour progression in HPV18-infected
101 (15) or HPV33-infected keratinocytes (16). A recent study investigated undifferentiated
102 keratinocytes containing HPV16 or HPV18 episomal genomes. However, no studies have
103 analysed how cellular gene expression is altered in differentiating keratinocytes supporting
104 the productive phase of the viral life cycle (17). Here we used Next Generation Sequencing
105 (RNASeq) to examine global changes in the keratinocyte transcriptome due to epithelial
106 differentiation and HPV infection. Our study reveals that HPV infection induces massive
107 changes in the transcriptome during keratinocyte differentiation. In particular, changes in
108 many genes encoding the keratinocyte structural barrier and immune function were altered.
109 Key statistically highly significant changes in gene expression were confirmed by RT-qPCR
110 and western blotting and investigated in clinical samples representing the cervical disease
111 spectrum. These data can be used to understand late events in the viral life cycle and the
112 mechanisms behind cervical disease progression.

113

114

115

116 **Results**

117 The HPV E2 transcription factor (18) and the viral oncoproteins E6 (19), E7 (20) and E5 (21)
118 can all play a role in controlling cellular gene expression, and HPV infection is known to have
119 a significant effect on keratinocyte growth and differentiation (6). In order to elucidate how
120 cellular gene expression is altered during HPV infection we examined changes in the
121 keratinocyte transcriptome during differentiation and HPV16 infection using normal,
122 spontaneously immortalised keratinocytes (NIKS) and the same cells stably transfected with
123 HPV16 genomes (NIKS16). NIKS16 clone 2L maintains ~100 episomal HPV16 genomes per
124 cell (if cultured at low passage (<13)) and forms a CIN1-like (low grade cervical disease)
125 stratified epithelium upon raft culture, suggesting that these cells represent a transient
126 HPV16 infection (22). We also examined a second HPV16 infection model, W12 cells, which
127 are HPV16-infected basal cervical epithelial cells isolated from a patient with a low grade
128 cervical lesion (23). W12 clone 20863 (W12E) cells (if cultured at low passage (<17)) also
129 maintain ~100 episomal HPV16 genomes (24). Both cell lines are capable of differentiation.
130 We used the differentiation protocol from Jeon et al (1995) where cells are induced to
131 differentiation by culturing to high density in 1.2 mM Ca⁺⁺. Differentiated NIKS16 and W12E
132 cell populations expressed involucrin, loricrin and keratin 10 proteins, key markers of
133 keratinocyte differentiation, (Figure 1A). NIKS16 cells (and W12 cells (25)) expressed viral
134 late proteins E2, E4 and L1 (Figure 1A, B). A time course of NIKS and NIKS16 differentiation
135 over a 13 day period is shown in Figure 1C. As expected, NIKS cells (Figure 1C lanes 1-4)
136 expressed more involucrin over the time course than NIKS16 cells (Figure 1C lanes 5-8)
137 because HPV infection impairs epithelial differentiation (6). Absolute quantification of viral
138 genome copies by PCR showed that differentiated W12 cells had an average of 15,250
139 genome copies while there was an average of 9937 copies NIKS16 cells (Figure 1D). Viral
140 late mRNA levels, as measured by L1 open reading frame detection, the common reading
141 frame in all late mRNAs, was increased 16.1-fold in W12 cells and 12.6-fold in NIKS16 cells

142 upon differentiation (Figure 1E). These data indicate that NIKS16 and W12 cells can be
143 differentiated in monolayer culture.

144 **Global changes in the transcriptome of HPV16-infected keratinocytes.**

145 RNASeq was carried out using RNA prepared from undifferentiated and differentiated NIKS
146 and NIKS16 populations. Comparing undifferentiated with differentiated uninfected NIKS,
147 809 mRNAs were up-regulated while 422 mRNAs were down-regulated (Figure 2A). In
148 contrast, comparing undifferentiated to differentiated HPV16-infected NIKS16 keratinocytes,
149 2041 genes were up-regulated while 2052 genes were down-regulated (Figure 2B). Because
150 NIKS16 cells are derived directly from NIKS (22) and were differentiated using the same
151 protocol, the 2862 additional changes observed upon differentiation of HPV16-positive
152 keratinocytes are likely attributable to HPV infection. A similar number of gene expression
153 changes to that for NIKS16 cells were observed between undifferentiated and differentiated
154 W12E cells (data not shown). There is no HPV-negative equivalent to W12 cells but we
155 compared the overlap of RNASeq changes in the transcriptome of differentiated W12 cells
156 compared to NIKS cells and NIKS16 cells compared to the parent NIKS cells. Despite the
157 fact that these cells are of different origin, W12 is a female HPV-immortalised mucosal
158 epithelial cell line while NIKS is a spontaneously male cutaneous epithelial cell line, there
159 was a 41% overlap in upregulated genes (Figure 2C) and a 38% overlap in downregulated
160 genes (Figure 2D). These data suggest that the effects of HPV infection and the
161 differentiation process is somewhat similar both cell types.

162

163 **HPV16 infection abrogates differentiation and epithelial barrier formation**

164 We are interested in elucidating the link between keratinocyte differentiation and late events
165 during HPV replication. Therefore, we compared the transcriptome of differentiated NIKS to
166 NIKS16 cells. Three, replicate, single-end sequencing experiments were carried out and
167 changes that gave a $p\text{-value} > 0.05$ across three replicates were discarded to achieve

168 significance. Supplementary Table S1 lists the top 966 changes in gene expression (
169 $p < 0.05$, $\log_2 > 1.8$, 3.5-fold change). 670 genes were downregulated while 296 were
170 upregulated, with a range of 184-fold downregulation to 87-fold up-regulated. The data in
171 Figure 3 shows the mean of the results of three separate RNASeq experiments. As
172 expected, key epithelial differentiation markers were down-regulated in NIKS16 cells (Figure
173 3A). Suprabasal layer keratins were also down-regulated. Keratin 12, which is usually only
174 expressed in the corneal epithelium (26), was the only keratin whose levels were increased
175 in NIKS16 cells (Figure 3B). Expression of cell junction proteins that are key to epithelial
176 barrier function was significantly altered. Desmosome cell-cell junction proteins required for
177 cell adhesion (Figure 3C) (27), and gap junction connexin (Cx) proteins 26, 30 and 32, that
178 allow transfer of small molecules between differentiating epithelial cells (28), were down-
179 regulated (Figure 3D). Claudin proteins control tight junctions, and CLDN3, 10 and 22 were
180 up-regulated while CLDN11 and 17 were down-regulated (Figure 3E). Claudin upregulation
181 can still have a negative impact on the function of tight junctions in a phenomenon referred
182 to as “leaky claudins” (29). Several adherens junction-associated cadherins (27) were also
183 down-regulated (Figure 3F). Small proline-rich repeat protein (SPRR) family members that
184 contribute to barrier formation by forming the cornified layer in differentiated epithelial cells
185 (30) were down-regulated (Figure 3G). The calcium gradient in the epithelium is altered upon
186 loss of barrier formation (31) and levels of RNAs encoding a range of calcium ion-binding
187 proteins (e.g. S100A8/A9 calgranulin complex, DSG1, matrix Gla protein (MGP),
188 calcium/calmodulin kinase 2B (CAMK2B)) were reduced (Supplementary Table S3). Taken
189 together, the data suggest that HPV infection inhibits epithelial barrier formation and
190 epithelial integrity.

191 The epithelial barrier also involves immune signalling and significant changes in expression
192 of many genes whose products are involved in intrinsic and innate immunity were also
193 observed (Table 1). Previously, a microarray study revealed that HR-HPV repressed
194 activation of the immune response in undifferentiated epithelial cells through IL-1 β . Similarly,

195 in HPV-infected differentiated cells we found IL1B gene expression was down-regulated.
196 IL1A was also down-regulated, as were IL32G and IL36B that activate keratinocyte immune
197 functions. The Langerhans cell chemoattractant CCL20 was down-regulated in the presence
198 of HPV16. However, CCL28 that controls T-cell homing in mucosal epithelia, E6/E7-
199 regulated CXCL12 and CX3CL1 were all up-regulated. The type 1 IFN regulator, IRF1 and
200 the epithelial IFN κ were up-regulated, an unexpected finding since HPVE6 and E7 have
201 been shown to inhibit their expression (32-34). We found a 6-fold down-regulation of the viral
202 DNA pattern recognition receptor TLR7, which is expressed specifically in differentiated
203 keratinocytes (35), together with up-regulation of viral restriction factors APOBEC3B, IFIT1,
204 2, 3 and 5, CD74, OASL and RTP4 (Table 1). These data indicate that the keratinocyte-
205 mediated immune response is under controlled of HPV16 in the upper epithelial layers, and
206 that there are significant differences to HPV-regulation of immune signalling in differentiated,
207 compared to basal, epithelial cells (17)

208

209 **Cellular networks involved in the immune response and keratinocyte structure and**
210 **metabolism are altered by HPV16 infection.**

211 Following adjustment of the data set to exclude any changes where the triplicate values
212 gave a p-value of >0.05 , gene ontology network pathway analysis of the top 1000 up or
213 down-regulated genes was carried out. Analysis revealed distinct gene classes whose
214 expression was altered by HPV16-infection (Figure 4). Response to type 1 interferon was
215 up-regulated but cytokine and chemokine expression was repressed. Cell matrix adhesion
216 was up-regulated while cell-cell adhesion was down-regulated (reported by the Cytoscape
217 programme as negative regulation of up-regulated leukocyte genes) (Figure 4A). Other
218 significantly down-regulated pathways included keratinization, arachidonic acid metabolism,
219 reactive oxygen and nitric oxide biosynthesis, VEGF and temperature homeostasis (Figure
220 4B). Network analysis indicated that pathways related to the type 1 interferon response were

221 strongly connected (Figure 4C) while down-regulated genes were associated through
222 cytokine/chemokine/VEGF pathways (Figure 4D). A value of \log_2 change >2.5 was chosen to
223 construct a wider pathway linkage diagram. IRF1 and KDR were major HPV-up-regulated
224 genes encoding hub proteins that connected a number of cell growth and apoptosis
225 signalling pathways. IL-1B and REL, an NFkB family transcriptional co-activator, linked HPV-
226 down-regulated cytokine and VEGF (Figure 5, Supplementary Table S3).

227

228 **Verification of gene expression changes due to HPV16 infection**

229 Six genes from among the most statistically highly significant changes (Table 2: padj values
230 are shown where $p=0.05$ in the triplicate data set is given the value of 1) were selected for
231 further study (negative: DSG1, SERPINB3, KRT10, positive: VTCN1, KDR, AZGP1).
232 Although IL1B had a padj =1 (actual p-value=0.05) it was also included because expression
233 of this important cytokine was found to be a key gene network hub in both undifferentiated
234 (17) and differentiated HPV-infected cells (Figure 5). These genes all encode proteins with
235 known metabolic or immune/inflammatory roles in the normal epithelium. KRT10 is a
236 differentiation-specific keratinocyte filament protein. DSG1 is a calcium-binding desmosome
237 regulator. KDR (vascular endothelial growth factor receptor 2, VEGFR-2) has an autocrine
238 function in cell proliferation, adhesion and migration (36). IL1B “node” cytokine activates
239 adaptive immunity. VTCN1 is a T-cell activation inhibitor. SERPINB3 controls epithelial
240 inflammatory responses and AZGP1 is induced by IFN γ in keratinocytes (37). mRNA
241 expression in NIKS versus NIK16 cells and W12 cells was validated by qRT-PCR (Table 2).

242 Protein levels encoded by these mRNAs were examined in undifferentiated and
243 differentiated NIKS, NIKS16 and W12 cells (Figure 6). Levels of AZGP1, KDR,
244 DSG1, KRT10, and involucrin increased upon NIKS16 and W12 cell differentiation, while
245 SERPINB3 levels decreased and VTCN1 levels did not change. Compared to differentiated
246 NIKS cells, there were higher levels of VTCN1, AZGP1 and KDR in NIKS16 cells but KRT10

247 and DSG1 levels were much lower in differentiated NIKS16, compare to NIKS cells, as
248 expected. SERPINB3 levels were greatly reduced following differentiation of NIKS16, but not
249 NIKS cells. There is no HPV-negative W12 cell equivalent to NIKS cells so it is not possible
250 to be sure if the changes in protein expression in W12 cells upon differentiation are due to
251 HPV infection. These data confirm that selected keratinocyte transcriptomic changes due to
252 HPV16 infection are reflected in protein levels.

253

254 **HPV16 infection-regulated mRNA as biomarkers of cervical disease**

255 It could be argued that the NIKS16 model of the HPV16 life cycle may not directly relate to
256 cervical HPV infection because NIKS16 cells are foreskin, not cervical, keratinocytes,
257 However, NIKS16 cells appeared to represent a low grade cervical lesion when grown in raft
258 culture (22) and the organisation of the HPV life cycle at different anatomical sites is quite
259 similar (38). HPV16-associated gene expression changes in keratinocytes could be related
260 to the productive life cycle but could equally be associated with cervical disease progression.
261 Therefore, to test whether any of the HPV-related changes in keratinocyte gene expression
262 we detected could have potential as HPV-associated cervical disease biomarkers, we
263 quantified levels of expression of three up- and three-down-regulated genes (two regulators
264 of the inflammatory response (IL1B, SERPINB3), two proteins involved in cell signalling
265 (KDR, VTCN1), and two involved in barrier function (KRT10, DSG)) by RT-qPCR in liquid
266 based cytology (LBC, Pap smear) samples. Apart from choice due to gene function, IL1B
267 RNA was chosen for analysis because it encoded a hub in the interactome (Figure 5),
268 VTCN1 and DSG1 were chosen as representative of very highly significantly altered RNAs,
269 KRT10 was chosen as a differentiation marker, KDR was chosen as an RNA potentially
270 involved in cancer formation and SERPINB3 was chosen because it was an early-identified
271 cervical cancer marker (39). Due to lack of mRNA we were unable to test AZGP1. A control
272 cDNA from differentiated W12E cervical keratinocytes was included in each qPCR plate as a

273 standard and absolute levels of RNA in the LBC samples (normalised against GAPDH) were
274 calculated using the Pfaffl standard curve method (40, 41). KRT17 was analysed as a known
275 biomarker of cervical disease progression (42). Figure 6 shows the mean and range of
276 values for each mRNA in 7 no detectable disease (NDD), 10 low grade cervical lesion
277 (CIN1) and 10 high grade cervical lesion (CIN3) samples. Although we analysed 10 samples
278 graded as NDD, once HPV typing status was revealed, 3 of these were HPV-positive. We
279 decided to exclude these from the analysis in order to compare HPV-negative with HPV-
280 positive clinical samples. KRT10 mRNA levels were very low making analysis of significance
281 difficult, and there was high variability in levels of IL1B and VTCN1. However, very high
282 levels of IL1B mRNA were detected in all patient samples, regardless of disease stage.
283 DSG1 was significantly increased between no detectable disease (NDD) and low grade
284 disease but significantly decreased between low grade and high grade disease. KDR and
285 SERPINB3 levels were significantly up-regulated between low grade and high grade
286 disease, similar to the positive control, KRT17. These data suggest that RNASeq analysis
287 has potential to uncover novel biomarkers of cervical disease.

288

289 **Discussion**

290 The aim of our work is to examine how human papillomavirus replication is linked to
291 keratinocyte differentiation. In particular we are interested in how differentiating keratinocytes
292 respond to HPV infection during the late, productive phase of the viral life cycle. As a model
293 to compare HPV-negative to HPV-positive keratinocytes, we used NIKS and NIKS16 cells.
294 NIKS are spontaneously immortalised neonatal foreskin keratinocytes that have no
295 alterations in differentiation or apoptosis (43). NIKS16 cells were derived directly from NIKS
296 cells by stable transfection of the HPV16 genome isolated from W12 cells (22). We have
297 shown that the NIKS16 cells adequately supported the infectious viral life cycle (as
298 previously reported (22)) because several key markers of keratinocyte differentiation and
299 viral life cycle completion: viral genome amplification, viral late mRNA induction and capsid
300 protein production, were detected. Moreover, because there was repression of VEGF
301 pathways, reduced expression of HOX and MMP proteins, and no general up-regulation of
302 EMT markers, these cells are likely not undergoing tumour progression. Because NIKS cells
303 are foreskin keratinocytes, they will likely have a number of differences in their gene
304 expression profile compared to cervical keratinocytes. We did not have access to
305 spontaneously immortalised HPV-negative cervical keratinocytes but we compared changes
306 in W12 gene expression with NIKS cells. There was around 40% identity in the up- and
307 down-regulated genes between NIKS16 and W12 cells. W12 cells are naturally infected,
308 female, mucosal epithelial cells while NIKS16 cells are male cutaneous epithelial cells and
309 spontaneously immortalised, and these significant differences likely account for the
310 remaining 60% of non-overlapping genes. Therefore, NIKS16 is potentially a more robust
311 model for HPV16-associated penile lesions than cervical lesions and it will be interesting in
312 future to compare these data sets with similar sets from differentiated uninfected and
313 infected cervical keratinocytes. 3D raft culture would undoubtedly provide a superior
314 approach for examining keratinocyte differentiation and HPV infection. However, for analysis
315 of late events in the viral life cycle in differentiated keratinocytes, this is technically

316 challenging, and difficult to reproduce, because RNA isolation from multiple, microdissected,
317 upper epithelial layer sections would be required for triplicate RNASeq experiments. Our
318 current dataset should provide an important basis for subsequent analysis of raft culture
319 models.

320

321 Many transcriptomic studies have analysed cellular changes during HPV-associated tumour
322 progression or due to overexpression of viral proteins (14, 15, 18, 21, 44-51). Of the
323 microarray studies investigating changes due to HPV infection, as opposed to
324 tumourigenesis, one compared expression of HPV31-positive and negative cervical
325 keratinocytes (14), a second examined HPV33-negative and positive vaginal keratinocytes
326 (16) while another compared undifferentiated anogenital keratinocytes with or without
327 episomal HPV16 and 18 genomes (17). All of these studies focused on the effect of HPV on
328 basal keratinocytes, the site of viral entry, and initial replication. No studies to date have
329 examined keratinocyte responses to late events in the viral replication cycle. Moreover, the
330 previous studies used microarray analysis which does not provide the unparalleled depth of
331 information available from RNASeq. To our knowledge, this is the first report comparing the
332 transcriptome of uninfected to HPV-infected differentiated keratinocytes using RNASeq. HPV
333 infection induced massive changes (2862 additional expression changes compared to HPV-
334 negative NIKS cells) in the keratinocyte transcriptome. Desmosomes, adherens, tight and
335 gap junction classes were all down-regulated in the presence of HPV16, likely due to HPV16
336 E6/E7 reactivation of the cell cycle and decreased keratinocyte differentiation (52) as has
337 been reported previously (17). Together with high level down-regulation of SPRRS, altered
338 arachidonic acid metabolism and changes in mucins (Supplementary Table S3), one can
339 conclude that HR-HPV infection results in a broad abrogation of epithelial barrier function
340 and epithelial integrity. Reduced barrier function could result in increased fragility of cells in
341 the upper epithelial layers to facilitate viral egress.

342

343 Keratinocytes are key players in the immune response, and they produce a panoply of
344 molecules involved in host defence against pathogens. In differentiated NIKS16
345 keratinocytes, HPV infection altered gene expression related to innate immunity, including
346 reduced expression of TLR7, IL1A, IL1B, NLRP3, IL36B, and IL32G. TLR7, a pattern
347 recognition receptor for viral nucleic acids, is upregulated upon keratinocyte differentiation
348 (35) and activates proinflammatory cytokines, and other molecules involved in the adaptive
349 immune response. There was a 6-fold down-regulation of TLR7 in the presence of HPV16
350 suggesting that the virus represses pattern recognition during vegetative viral genome
351 amplification, but by a different mechanism to that used in undifferentiated keratinocytes
352 where infection suppresses TLR9 (17). There was a corresponding reduction in NFkB-
353 regulated CCL20, known to be regulated by HPV E7 (53), and required to recruit
354 Langerhans cells. Indeed, NFkB signalling was affected and the NFkB family member, REL,
355 was a major HPV-regulated control node in the pathway analysis of negatively regulated
356 genes (Supplementary Figure 1). Surprisingly, we discovered that the epithelial-specific
357 IFN κ , and IRF1 that controls type 1 IFNs, were up-regulated by HPV16 in differentiated
358 keratinocytes. Previously, HPV16 E7 or HPV38 E6E7 were shown to inhibit IRF1 expression
359 (32, 33), while HPV16 E6 was shown to repress IFN κ transcription through promoter
360 methylation (54). However, these studies used overexpression of the viral oncoproteins. The
361 levels of E6 or E7 proteins may be much lower in differentiated keratinocytes compared to
362 that in the undifferentiated epithelial cells or cervical cancer cells used in these studies. In
363 contrast to E6 and E7, E5 can stimulate IRF1 expression in HaCaT cells (55). Changes due
364 to expression of the entire virus genome may be more complex and quite different to that
365 seen with expression of individual viral proteins. Up-regulation of IFITs corresponded with
366 the observed activation of the type 1 interferon response. Only IFIT1 has been shown to
367 inhibit HPV replication (56, 57) therefore, the roles of other IFITs in inhibiting HPV infection
368 remain to be determined. APOBEC3B was up-regulated however, we found no changes in
369 expression of APOBEC3A, a known HPV restriction factor, but its expression may be
370 differentially regulated only in less differentiated keratinocytes (58). The observed up-

371 regulation of CXCR6 and CXCL12 is in agreement with CXCL12 detection in HPV-induced
372 lesions and its role in the productive HPV life cycle (59). We also detected changes in some
373 SERPINs (e.g. SERPINB3) that are involved in the inflammatory/immune response (60). We
374 did not detect changes in STAT1 that has been shown to be controlled by E6 and E7 (61).
375 It is possible that it undergoes changes of less than the cut-off of >3.5-fold considered here.
376 However, STAT1 controls IRF1 expression, which was upregulated 4-fold and STAT1 was a
377 central node connecting gene pathways regulated by HPV16 (Supplementary Figure 1). Of
378 course, because we used an immortal cell line, immortalisation could account for some of
379 the changes we observed. It will be important to analyse innate immune regulators in
380 differentiated primary cervical keratinocytes in future studies. Our data reveal that HPV
381 suppression of intrinsic and innate immunity takes place not only in infected basal epithelial
382 cells (17) but also in keratinocytes harbouring late events in the HPV life cycle, and that a
383 differentiation stage-specific set of events may be relevant to this life cycle stage. The
384 stimulation of the IFN response and viral restriction factors in differentiated HPV-infected
385 cells requires further study. Production of progeny viral genomes and virions may stimulate
386 the IFN response and lead to apoptosis and this could aid release and dissemination of virus
387 particles.

388

389 The E5, E6, E7 and E2 proteins of HPV 16 are known to control cellular gene expression. E6
390 and E7 control keratinocyte cell cycle and apoptosis and abrogate differentiation. Many of
391 the changes in gene expression we have observed can be attributed to these functions of
392 the viral oncoproteins. These changes are clearly important for the replicative life cycle of
393 HPV16 but could also contribute to HPV persistence and development of neoplasia (6).
394 Similar to data from one overexpression study of HPV16 E6 in human foreskin keratinocytes
395 (50), the differentiation marker involucrin, vimentin that is expressed upon epithelial stress,
396 and signal transduction proteins MEST and H19, were up-regulated in our analysis.
397 However, we detected none of the other changes affecting cell cycle, proliferation, DNA
398 damage, metabolism or signalling that have previously been reported (50). We discovered

399 only 7 genes (Semaphorin 5A (SEMA5A), CXCL1, ENTPOT, Follistatin (FST), Cytochrome
400 P450 (CYP) 24A1, Pleckstrin homology-like domain A1 (PHLDA1) and ribosomal proteins
401 S27-like (RPS27L)) out of a total of 99 altered in another study using siRNA depletion of E6
402 in HPV-positive tumour cells (47). Compared to a study of W12 cells with integrated HPV16
403 genomes expressing different levels of E6 and E7, we detected E6-regulated loricrin (LOR)
404 and cytochrome P450 (CYP) 1B1, and E7-regulated FABP4, SERPINA3, SLURP1 out of the
405 top 20 genes up-regulated by each protein (62). Only one out of 12 master regulators of E6
406 or E7 function defined by Smith et al (62) was in common with our study. This was
407 downregulation of PRDM1 (BLIMP-1) which acts as a repressor of IFN- β gene expression.
408 E5 overexpression in HaCaT keratinocytes yielded 61 mRNAs with significant changes (21)
409 but only two of these (Keratin 8, MMP16) were in common with our RNASeq data. In a
410 microarray study of E2 overexpression in U2OS cancer cells where 74 genes were found to
411 be regulated, only 3 of these (heterotrimeric G-complex protein 11 (GNG11) involved in cell
412 signalling, histamine N-methyltransferase (HNMT) involved in methylation of histamine and
413 SERPINA3 which is up-regulated in response to decreased transglutaminase activity) were
414 altered in our study. Increased viral oncoprotein expression levels in HPV-positive cancer
415 cells, or in cells overexpressing viral proteins, compared to the model we have used, i.e.
416 keratinocytes supporting expression of all viral proteins from the intact HPV16 genome
417 where expression levels are much lower (3), could explain the fact that we did not detect
418 many of these changes. Moreover, we have only considered expression changes >3.5-fold,
419 while these other studies considered 2-fold changes. RNASeq analysis of the W12 tumour
420 progression series (63) would help to delineate infection versus cancer-related changes.

421

422 Liquid based cytology samples (LBCs, Pap smear samples) contain cells scraped from the
423 top of the cervical epithelium and thus contain HPV-infected differentiated keratinocytes.
424 Therefore, some of the mRNA changes we have detailed could be biomarkers of cervical
425 disease. Very high levels of IL1B mRNA were detected in all patient samples, regardless of
426 disease stage, likely due to inflammation commonly observed in diseased cervix. Statistically

427 significant changes in KDR and SERPINB3 expression, like the known biomarker KRT17,
428 indicate their potential in identifying high grade cervical disease. DSG1 was significantly
429 increased between no detectable disease (NDD) and low grade disease but significantly
430 decreased between low grade and high grade disease. This is in contrast to the clear down-
431 regulation of DSG1 expression due to HPV16 infection of NIKS and suggests either that
432 NIKS16 cells may not represent a low grade HPV16-positive lesion or that the levels of
433 DSG1 in cervical keratinocytes is very different to that in foreskin keratinocytes.

434

435 In conclusion, we report for the first time RNASeq analysis of changes in the keratinocyte
436 transcriptome caused by HR-HPV infection. Infection caused massive changes in epithelial
437 gene expression. These changes showed mainly a profile expected of viral infection, rather
438 than tumour progression. The large dataset we have developed opens up the possibility of a
439 deeper understanding of late events in the HPV replication cycle in response to keratinocyte
440 differentiation. As well as shedding light on late events during the HPV16 life cycle, the
441 RNASeq data could uncover potential biomarkers of HPV-associated anogenital disease
442 progression. From our analysis, DSG1, KDR and SERPINB3 expression may have potential
443 as robust markers that can risk-stratify cervical disease, i.e. identify cervical disease cases
444 that have a high probability of regression, and this would be of significant clinical value.
445 However, further longitudinal studies where biomarker status is linked to clinical outcomes
446 would be required to validate any biomarkers for such an application.

447

448 **Materials and Methods**

449 **Clinical sample panel underlying pathology and HPV status**

450 Anonymised, cervical liquid based cytology samples were obtained from the Scottish
451 National HPV archive which holds Generic Scotland A Research Ethics Committee approval
452 for Research Tissue banks (REC Ref 11/AL/0174) for provision of samples for HPV related
453 research after approval from an independent steering committee. The Scottish HPV Archive
454 also comes under the auspice of the NHS Lothian Bioresource. The panel comprised HPV
455 negative/cytology negatives samples (no disease, n=7) samples with low-grade cytological
456 abnormalities with histological confirmation of cervical intraepithelial neoplasia (CIN) 1 (low-
457 grade disease, n=10) and samples with high-grade cytological abnormalities with histological
458 confirmation of CIN2 or worse, including cancer (high-grade disease, n=10). Cytology
459 grades were reported according to the British Society for Clinical Cytopathology (BSCC)
460 classification (64-66). HPV testing was performed by the Optiplex HPV genotyping Assay
461 (Diamex, Heidelberg, Germany) according to manufacturer's instructions. The Optiplex test
462 is a PCR based assay which uses a luminex platform for the detection of 24 individual HPV
463 types including all established as high-risk according to the International Agency on
464 Research on Cancer. For the purposes of this panel, the main function of the genotyping
465 was for the annotation of no disease "controls". Women with negative cytology and HPV
466 negative status are at a very low risk of underlying disease (negative predictive value for a
467 high grade lesion of >95% (67)) All experiments were performed in compliance with relevant
468 laws and institutional guidelines and in accordance with the ethical standards of the
469 Declaration of Helsinki.

470

471 **Cell lines**

472 W12E (24), NIKS (43), and NIKS16 cells (22) were co-cultured in E-medium with mitomycin
473 C-treated J2 3T3 fibroblast feeder cells as previously described (24). Differentiation was
474 induced by growth to high density in 1.2 mM Ca⁺⁺ (24). 3T3 cells were grown in DMEM with

475 10% donor calf serum. Prior to harvesting, 3T3 cells were removed by trypsinisation and
476 cells layers washed twice with PBS. All cells were maintained under humidified 5% CO₂ 95%
477 air at 37°C.

478 **RNA isolation – cell lines**

479 Protocols followed the manufacturer's instructions. Total RNA was prepared using Qiagen
480 RNeasy kit. RNA was quantified by measuring the ratio of absorbance at 260 and 280 nm
481 using a Nanodrop ND-1000 spectrophotometer (ThermoScientific). Polyadenylated RNA was
482 prepared using an oligo-dT-based mRNA extraction kit (Oligotex, Qiagen).

483 **RNA isolation – clinical samples**

484 LBC cells in 4ml in PreservCyt collection medium (Cytoc Corporation) were pelleted by
485 centrifugation in a Beckman GPR bench top centrifuge at 1500g for 10 min. The cell pellet
486 washed with sterile PBS. RNA extraction was carried out using the RNeasy miRNA
487 preparation kit (Qiagen). RNA was quantified and purity assessed by measuring the ratio of
488 absorbance at 260 and 280 nm using a Nanodrop ND-1000 spectrophotometer.

489 **qRT-PCR**

490 For cell line and clinical samples, DNA was removed using Maxima DNase and treated RNA
491 was reverse transcribed using Maxima First Strand cDNA synthesis kit according to
492 manufacturer's instructions (ThermoScientific). Standard curves were generated as
493 recommended (Applied Biosystems instruction manual). Triplicate amplification reactions
494 containing 100 ng cDNA each were carried out. GAPDH and β -actin were used as the
495 internal standard controls. Probes and primers are: GAPDH F: 5'-
496 GAAGGTGAAGGTCGGAGT-3', GAPDH R: 5'- GAAGATGGTGATGGGATTTTC-3', GAPDH
497 Probe: 5'-CAAGCTTCGTTCTCAGCC. KRT10F: 5'- TGGTTCTTGCCCTCAGAAGAGCTGA-
498 3', KRT10 R: 5'- AGTACACGGTGGTGTCTGTGTCAT-3', KRT10 Probe:
499 TGTGTCCACTGGTGATGGGAATGTGG-3'. DSG1 F: 5'- ACGTTCACGATAACCGACCAGC

500 AT-3', DSG1 R: 5'- ATTCCATGCAAATCACGGCCAGAG-3', DSG1 Probe: 5'- AACGTGGT
501 AGTGACAGAGAGAGTGGT-3'. KDR F: 5'- TGGTTCTTGCCTCAGAAGAGCTGA-3', KDR
502 R: 5'- AGTACACGGTGGTGTCTGTGTCAT-3', KDR Probe: 5'-
503 TGGCATCTGAAAGCTCAAACC
504 AGACA-3'. IL1B F: 5'- TCTGTACCTGTCCTGCGTGTGAA-3', IL1B R: 5'- TGCTTGAGAGG
505 TGCTGATGTACCA-3', IL1B Probe: 5'- CAAGCTGGAATTTGAGTCTGCCAGT-3'. VTCN1
506 F: 5'-CACCAGGATAACATCTCTCAGTGAA-3', VTCN1 R: 5'- TGGCTTGCAGGGTAGAATG
507 A-3', VTCN1 Probe: 5'- AAGCTGAAGATAATCCCATCAGGCAT-3'. SERPINB3 F: 5'-
508 GCTGC
509 CAAATGAAATCGATGGTCTCC-3', SERPINB3 R :5'- TTCCCATGGTTCTCAACGTGTCCT-
510 3', SERPINB3 Probe: 5'-AACTCGGTTCAAAGTGGAAAGAGAGCT-3'. KRT17 F: 5'- GATGC
511 GTGACCAGTATGAGAAG-3', KRT17 R: 5'- CGGTTCAAGTTCCTCTGTCTTG-3', KRT17
512 Probe: 5'- ATGGCAGAGAAGAACCGCAAGGAT-3'. Reaction mixes (25 µl) contained 1x
513 Mastermix (Stratagene), 900 nM primers, 100 nM probe, 300 nM reference dye
514 (Stratagene). qPCR reactions were performed and analysed on an Applied Biosystems
515 7500 Fast System. Graphing and statistical analyses were performed using GraphPad Prism
516 7. Statistical analysis (all three groups were compared to each other) was performed by
517 Kruskal-Wallis test and data analysed by one way ANOVA with Tukey's post-test. A
518 significance level of $p < 0.05$ was used.

519 **Western blot analysis**

520 Cells were lysed in 2 x protein loading buffer (125 mM Tris (pH 6.8), 4% SDS, 20% glycerol,
521 10% mercaptoethanol and 0.006% bromophenol blue with fresh protein inhibitor cocktail
522 (Roche, UK)). Protein extracts were syringe-passaged through a 22-gauge needle 15 times
523 then sonicated in a Sonibath for three 30 sec pulses to break up DNA strands. The samples
524 were boiled at 100°C for 5 min before loading on a 12% Novex gel (Invitrogen) and
525 electrophoresed at 150V for 1 hour in 1X MES buffer. Gels were transferred to a
526 nitrocellulose membrane using the iBlot transfer kit and iBlot Gel Transfer Stacks (Invitrogen)

527 as per the manufacturer's instructions. Membranes were blocked in 5% milk powder in PBST
528 at room temperature for at least one hour. Membranes were washed 3 times in PBST for 5
529 minutes each then incubated with primary antibody. Mouse monoclonal antibodies, GAPDH
530 (Meridian, 6C5), involucrin (Sigma, I9018), loricin (Abcam, ab85679), serpinB3 (Sigma,
531 2F5) and keratin 10 (Abcam, ab9026) were used at a dilution of 1:1000. HPV16 E2 antibody
532 (Santa Cruz, TVG261) was used at 1:500 dilution. HPV16 L1 antibody (Dako, K1H8) was
533 used at 1:400 dilution. HPV16 E4 antibody (Gift of J. Doorbar, Cambridge, UK, clone B11)
534 was used at a dilution of 1:50. Rabbit polyclonal antibodies DSG1 (Abcam, ab133662),
535 VEGFR2 (KDR) (Abcam, ab39256). AZGP1 (Invitrogen PA5-44912) were used at 1:1,000
536 dilution. VTCN1 (Proteintech, 12080-1-AP) was used a a dilution of 1:500. The blots were
537 incubated in their respective antibody for 1 hour at room temperature or overnight at 4°C.
538 After 1 hour, the blots were washed 3 times in PBS-T for 5 min. They were then placed in
539 secondary antibody for 1 hour (HRP-linked goat anti-mouse or goat anti-rabbit (Pierce) were
540 used at 1:2000 dilution. Blots were washed 3 times in PBST for 5 minutes before being
541 incubated with ECL western blot substrate. The blots were exposed to X-ray film
542 (ThermoScientific) and processed in an X-Omat processor.

543

544 ***Illumina sequencing***

545 Integrity of RNAs was assessed using an Agilent 2100 Bioanalyser. cDNA was synthesised
546 using reagents from the TruSeq RNA Sample Preparation kit (Illumina) according to the
547 manufacturer's instructions. cDNA libraries were sequenced with a 73 base single-end read
548 on an Illumina Genome Analyser IIx at the Glasgow Polyomics facility at the University of
549 Glasgow. Samples have been submitted to SRA@ncbi.nih.gov. STUDY: PRJNA379358
550 (SRP104232). SAMPLE: NIKS16_D11_Mar17 (SRS2131727), EXPERIMENT: Differentiated
551 NIKS16 cells (SRX2745325) RUN: NIKS_HPV16_D11_Mar17.fq.gz (SRR5457256).
552 SAMPLE: NIKS16_D5_Mar17 (SRS2131728), EXPERIMENT: Undifferentiated NIKS16 cells

553 (SRX2745326), RUN: NIKS_HPV16_D5_Mar17.fq.gz (SRR5457258). SAMPLE:
554 NIKS_D11_Mar17 (SRS2131729), EXPERIMENT: Differentiated NIKS cells (SRX2745327),
555 RUN: NIKS_D11_Mar17.fq.gz (SRR5457259). SAMPLE: NIKS_D5_Mar17 (SRS2131730),
556 EXPERIMENT: Undifferentiated NIKS cells (SRX2745328), RUN: NIKS_D5_Mar17.fq.gz
557 (SRR5457260)

558

559 **Computational analysis**

560 Datasets were cleaned of reads with runs > 12Ns. Alignment to the human cDNA set
561 (145,786 cDNAs – downloaded on 28th November 2011) was performed using Bowtie
562 version 0.12.7. Further alignment to an updated human cDNA set (180,654 cDNAs
563 downloaded April 30th 2012) was carried out using BWA 0.7.12-r1039. DESeq implemented
564 in BioConductor (68) was used to select cellular genes whose expression was up or down-
565 regulated by HPV in NIKS16 compared to NIKS cells implemented in the R environment.
566 The raw read counts were normalised using (RPKM). DESeq uses a negative binomial error
567 distribution to model transcript abundance and determine the differential expression. The
568 significance of differential expression was estimated for each gene and then corrected for
569 multiple comparisons (Padj). The top 1000 differentially expressed genes based on log-fold
570 change (Log₂FoldChange) of >1.8 (3.5-fold change) are listed in Supplementary Table S3.

571 **Functional analysis of differentially expressed genes**

572 GO (69) and KEGG (70) enrichment analyses were performed using Cytoscape
573 (<http://cytoscape.org/>) with ClueGO (Version 2.3.2) (71). The statistical test used for the
574 enrichment was based on a two-sided hypergeometric option with a Bonferroni step-down
575 correction, a *P*-value less than 0.05 and a kappa score of 0.4.

576

577 **Acknowledgements**

578 We thank Dr John Doorbar (University of Cambridge) for providing the NIKS and NIKS16
579 cells lines and Prof Margaret Stanley (University of Cambridge) and Prof Paul Lambert
580 (University of Wisconsin) for the W12 cell line. This work was funded by a grant to SVG from
581 the Wellcome Trust (088848/2/09/2) and to TK and SVG from Tenovus Scotland (S11/33).
582 We acknowledge funding from the Medical Research Council as core funding for the MRC
583 University of Glasgow Centre for Virus Research.

584

585

586 **Declaration of Conflicts of Interest**

587 We declare no conflicts of interest.

588

589 Table 1. Changes in expression of immune regulatory molecules and viral restriction factors.

Gene ID	Category	Negative fold change	Positive fold change
TLR7	PRR	6-fold	
NLRP3	Inflammasome component	7-fold	
IL1A	Cytokine	7-fold	
IL1B	Cytokine	4-fold	
IL32G	Cytokine	17-fold	
IL36B	Cytokine	6-fold	
CCL20	Chemokine	7-fold	
CCL28	Chemokine		5-fold
CXCL12	Chemokine		4-fold
CX3CL1	Chemokine		32-fold
APOBEC3C	Restriction factor		4-fold
IFIT1	Restriction factor		6-fold
IFIT2	Restriction factor		7-fold
IFIT3	Restriction factor		7-fold
IFIT5	Restriction factor		4-fold
CD74	Restriction factor		4-fold
AOSL	Restriction factor		4-fold
RTP4	Restriction factor		13-fold
IRF1	IFN regulatory transcription factor		4-fold
IFNk	Interferon kappa		8-fold

590

591

592 PRR: pattern recognition receptor. IFN, interferon.

593

594

595 Table 2. RNASeq expression changes in mRNAs of statistical significance ($p < 0.025$) verified
 596 by qPCR

Gene ID	Padj	NIKS16/NIKS- fold change RNASeq	NIKS16/NIKS- fold change qPCR	W12/NIKS- fold change qPCR	Gene Function
DSG1	2.05 $\times 10^{-5}$	-19.95	-4.20	-3.52	Desmoglein1: calcium-binding desmosome regulator
IL1B	1	-8.68	-5.65	-7.73	Interleukin 1b: inflammatory response regulator
SERPINB3	0.008	-8.40	-4.28	-4.410	Intracellular protease inhibitor, inhibits active inflammatory response
KRT10	0.021	-7.07	-10.26	-3.70	Keratin10: epithelial cytofilament
KDR	0.025	10.21	10.10	4.30	VEGFR-2, tyrosine kinase receptor
VTCN1	1.4 x 10^{-9}	46.12	8.94	10.56	V-set domain-containing T-cell activation inhibitor-1
AZGP1	2.05 $\times 10^{-5}$	12.64	7.49	8.31	Zinc alpha-2 glycoprotein: lipid metabolism
GAPDH		1	1	1	Glyceraldehyde-3-phosphate dehydrogenase (control)
Beta-actin		1	1	1	Actin (control)

597

598

599 **Reference List**

- 600 1. **zur Hausen H.** 2009. Papillomaviruses in the causation of human cancers - a brief
601 historical account. *Virology* **384**:260-265.
- 602 2. **Stanley MA.** 2012. Epithelial cell responses to infection with human papillomavirus.
603 *Clin. Microbiol. Rev.* **25**:215-222.
- 604 3. **Doorbar J, Egawa N, Griffin H, Kranjec C, Murakami I.** 2015. Human
605 papillomavirus molecular biology and disease association. *Rev. Med. Virol.* **25**:2-23.
- 606 4. **Wakeham K, Kavanagh K.** 2014. The burden of HPV-associated anogenital
607 cancers. *Curr. Oncol. Rep.* **16**:1-11.
- 608 5. **Gillison ML, Chaturvedi AK, Anderson WF, Fakhry C.** 2015. Epidemiology of
609 human papillomavirus–positive head and neck squamous cell carcinoma. *J. Clin.*
610 *Oncol.* **33**:3235-3242.
- 611 6. **Egawa N, Egawa K, Griffin H, Doorbar J.** 2015. Human papillomaviruses; epithelial
612 tropisms, and the development of neoplasia. *Viruses* **7**:2802.
- 613 7. **Pett M, Coleman N.** 2007. Integration of high-risk human papillomavirus: a key event
614 in cervical carcinogenesis? *J. Pathol.* **212**:356-367.
- 615 8. **Fuchs E, Byrne C.** 1994. The epidermis: rising to the surface. *Curr Opin Gen Dev*
616 **4**:725-736.
- 617 9. **Doorbar J.** 2005. The papillomavirus life cycle. *J Clin Virol* **32S**:S7-S15.
- 618 10. **Graham SV.** 2006. Late events in the life cycle of human papillomaviruses, p 193-
619 212. *In* Campo MS (ed), *Papillomavirus research: from natural history to vaccines*
620 *and beyond*, 1st ed. Caister Academic Press, Wymondham, Norfolk.
- 621 11. **Matsui T, Amagai M.** 2015. Dissecting the formation, structure and barrier function
622 of the stratum corneum. *International Immunology* **27**:269-280.
- 623 12. **Partidos CD, Muller S.** 2005. Decision-making at the surface of the intact or barrier
624 disrupted skin: potential applications for vaccination or therapy. *Cell. Mol. Life Sci.*
625 *CMLS* **62**:1418-1424.

- 626 13. **Westrich JA, Warren CJ, Pyeon D.** 2017. Evasion of host immune defenses by
627 human papillomavirus. *Virus Res.* **231**:21-33.
- 628 14. **Chang YE, Laimins LA.** 2000. Microarray analysis identifies interferon-inducible
629 genes and Stat-1 as major transcriptional targets of human papillomavirus type 31. *J*
630 *Viro* **74**:4174-4182.
- 631 15. **Karstensen B, Poppelreuther S, Bonin M, Walter M, Iftner T, Stubenrauch F.**
632 2006. Gene expression profiles reveal an upregulation of E2F and downregulation of
633 interferon targets by HPV18 but no changes between keratinocytes with integrated or
634 episomal viral genomes. *Virology* **353**:200-209.
- 635 16. **Ruutu M, Peitsaro P, Johansson B, Syrjänen S.** 2002. Transcriptional profiling of a
636 human papillomavirus 33-positive squamous epithelial cell line which acquired a
637 selective growth advantage after viral integration. *Int. J. Cancer* **100**:318-326.
- 638 17. **Karim R, Meyers C, Backendorf C, Ludigs K, Offringa R, van Ommen G-JB,**
639 **Melief CJM, van der Burg SH, Boer JM.** 2011. Human papillomavirus deregulates
640 the response of a cellular network comprising of chemotactic and proinflammatory
641 genes. *PLoS ONE* **6**:e17848.
- 642 18. **Gauson EJ, Windle B, Donaldson MM, Caffarel MM, Dornan ES, Coleman N,**
643 **Herzyk P, Henderson SC, Wang X, Morgan IM.** 2014. Regulation of human
644 genome expression and RNA splicing by human papillomavirus 16 E2 protein.
645 *Virology* **468–470**:10-18.
- 646 19. **Vande Pol SB, Klingelutz AJ.** 2013. Papillomavirus E6 oncoproteins. *Virology*
647 **445**:115-137.
- 648 20. **Roman A, Munger K.** 2013. The papillomavirus E7 proteins. *Virology* **445**:138-168.
- 649 21. **Kivi N, Greco D, Auvinen P, Auvinen E.** 2007. Genes involved in cell adhesion, cell
650 motility and mitogenic signaling are altered due to HPV 16 E5 protein expression.
651 *Oncogene* **27**:2532-2541.
- 652 22. **Weschler EI, Wang Q, Roberts I, Pagliarulo E, Jackson D, Untersperger C,**
653 **Coleman N, Griffin H, Doorbar J.** 2012. Reconstruction of human papillomavirus

- 654 type 16-mediated early-stage neoplasia implicated E6/E7 deeregualtion and the loss
655 of contact inhibition in neoplastic progression. *J Virol* **86**:6358-6364.
- 656 23. **Stanley MA, Browne HM, Appleby M, Minson AC.** 1989. Properties of a non-
657 tumorigenic human cervical keratinocyte cell line. *Int J Cancer* **43**:672-676.
- 658 24. **Jeon S, Allen-Hoffman BL, Lambert PF.** 1995. Integration of human papillomavirus
659 type 16 into the human genome correlates with a selective growth advantage of cells.
660 *J Virol* **69**:2989-2997.
- 661 25. **Milligan SG, Veerapraditsin T, Ahamat B, Mole S, Graham SV.** 2007. Analysis of
662 novel human papillomavirus type 16 late mRNAs in differentiated W12 cervical
663 epithelial cells. *Virology* **360**:172-181.
- 664 26. **Bragulla HH, Homberger DG.** 2009. Structure and functions of keratin proteins in
665 simple, stratified, keratinized and cornified epithelia. *J Anat* **214**.
- 666 27. **Bazzi H, Christiano AM.** 2007. Broken hearts, woolly hair, and tattered skin: when
667 desmosomal adhesion goes awry. *Curr. Opin. Cell Bio.* **19**:515-520.
- 668 28. **Laird D.** 2006. Life cycle of connexins in health and disease. *Biochem J* **394**:527-
669 543.
- 670 29. **Findley MK, Koval M.** 2009. Regulation and roles for claudin-family tight junction
671 proteins. *IUBMB Life* **61**:431-437.
- 672 30. **Carregaro F, Stefanini ACB, Henrique T, Tajara EH.** 2013. Study of small proline-
673 rich proteins (SPRRs) in health and disease: a review of the literature. *Arch.*
674 *Dermatol. Res.* **305**:857-866.
- 675 31. **Bikle DD, Oda Y, Xie Z.** 2004. Calcium and 1,25(OH)₂D: interacting drivers of
676 epidermal differentiation. *J. Steroid Biochem. .Mol. Biol.* **89-90**:355-360.
- 677 32. **Park J-S, Kim E-J, Kwon H-J, Hwang E-S, Namkoong S-E, Um S-J.** 2000.
678 Inactivation of interferon regulatory factor-1 tumor suppressor protein by HPV E7
679 oncoprotein: implication for the E7-mediated immune evasion mechanism in cervical
680 carcinogenesis. *J. Biol. Chem.* **275**:6764-6769.

- 681 33. **Cordano P, Gillan V, Bratlie S, Bouvard V, Banks L, Tommasino M, Campo MS.**
682 2008. The E6E7 oncoproteins of cutaneous human papillomavirus type 38 interfere
683 with the interferon pathway. *Virology* **377**:408-418.
- 684 34. **Ronco LV, Karpova AY, Vidal M, Howley PM.** 1998. Human papillomavirus 16 E6
685 oncoprotein binds to interferon regulatory factor-3 and inhibits its
686 transcriptional activity. *Genes Dev.* **12**:2061-2072.
- 687 35. **Li ZJ, Sohn K-C, Choi D-K, Shi G, Hong D, Lee H-E, Whang KU, Lee YH, Im M,**
688 **Lee Y, Seo Y-J, Kim CD, Lee J-H.** 2013. Roles of TLR7 in activation of NF- κ B
689 signaling of keratinocytes by imiquimod. *PLOS ONE* **8**:e77159.
- 690 36. **Man X-Y, Yang X-H, Cai S-Q, Yao Y-G, Zheng M.** 2006. Immunolocalization and
691 expression of vascular endothelial growth factor receptors (VEGFRs) and neuropilins
692 (NRPs) on keratinocytes in human epidermis. *Mol. Med.* **12**:127-136.
- 693 37. **Brysk MMB, T.; Hoida, C.; Tyring, S.K.; Rajaraman, S.** 1991. Interferon-gamma
694 modulates terminal differentiation and the expression of desquamin in cultured
695 keratinocytes. *Exp Cell Res* **197**:7.
- 696 38. **Peh W, L., Middleton K, Christensen N, Nicholls P, Egawa K, Sotlar K,**
697 **Brandsma J, Percival A, Lewis J, Liu WJ, Doorbar J.** 2002. Life cycle
698 heterogeneity in animal models of human papillomavirus-associated disease. *J Virol*
699 **76**:10411-10416.
- 700 39. **Kato, H, Torigoe T.** 1977. Radioimmunoassay for tumour antigen of human cervical
701 squamous cell carcinoma. *Cancer* **40**:8.
- 702 40. **Bustin SA, Beaulieu J-F, Huggett J, Jaggi R, Kibenge FSB, Olsvik PA, Penning**
703 **LC, Toegel S.** 2010. MIQE précis: Practical implementation of minimum standard
704 guidelines for fluorescence-based quantitative real-time PCR experiments. *BMC Mol*
705 *Biol* **11**:74.
- 706 41. **Pfaffl MW.** 2001. A new mathematical model for relative quantification in real-time
707 RT-PCR. *Nucleic Acids Res* **29**:e45-e45.

- 708 42. **Escobar-Hoyos LF, Yang J, Zhu J, Cavallo J-A, Zhai H, Burke S, Koller A, Chen**
709 **EI, Shroyer KR.** 2014. Keratin 17 in premalignant and malignant squamous lesions
710 of the cervix: proteomic discovery and immunohistochemical validation as a
711 diagnostic and prognostic biomarker. *Mod Pathol* **27**:621-630.
- 712 43. **Allen-Hoffmann BL, Schlosser SJ, Ivarie CAR, Meisner LF, O'Connor SL, Sattler**
713 **CA.** 2000. Normal growth and differentiation in a spontaneously immortalized near-
714 diploid human keratinocyte cell line, NIKS. *J Invest Dermatol* **114**:444-455.
- 715 44. **Chen J, Xue Y, Poidinger M, Lim T, Chew SH, Pang CL, Abastado J-P, Thierry F.**
716 2014. Mapping of HPV transcripts in four human cervical lesions using RNAseq
717 suggests quantitative rearrangements during carcinogenic progression. *Virology*
718 **462–463**:14-24.
- 719 45. **Nees M, Geoghegan JM, Munson P, Prabhu V, Liu Y, Androphy E, Woodworth**
720 **CD.** 2000. Human papillomavirus type 16 E6 and E7 proteins inhibit differentiation-
721 dependent expression of transforming growth factor- β 2 in cervical keratinocytes.
722 *Cancer Res* **60**:4289-4298.
- 723 46. **Nees M, Geoghegan JM, Hyman T, Frank S, Miller L, Woodworth CD.** 2001.
724 Papillomavirus type 16 oncogenes downregulate expression of interferon-responsive
725 genes and upregulate proliferation-associated and NF- κ B-responsive genes in
726 cervical keratinocytes. *J Virol* **75**:4283-4296.
- 727 47. **Kelley ML, Keiger KE, Lee CJ, Huibregtse JM.** 2005. The global transcriptional
728 effects of the human papillomavirus E6 protein in cervical carcinoma cell lines are
729 mediated by the E6AP ubiquitin ligase. *J Virol* **79**:3737-3747.
- 730 48. **Sopov I, Sørensen T, Magbagbeolu M, Jansen L, Beer K, Kühne-Heid R,**
731 **Kirchmayr R, Schneider A, Dürst M.** 2004. Detection of cancer-related gene
732 expression profiles in severe cervical neoplasia. *Int J Cancer* **112**:33-43.
- 733 49. **Chen Y, Miller C, Mosher R, Zhao X, Deeds J, Morrissey M, Bryant B, Yang D,**
734 **Meyer R, Cronin F, Gostout BS, Smith-McCune K, Schlegel R.** 2003.

- 735 Identification of cervical cancer markers by cDNA and tissue microarrays. *Cancer*
736 *Res* **63**:1927-1935.
- 737 50. **Duffy CL, Phillips SL, Klingelutz AJ.** 2003. Microarray analysis identifies
738 differentiation-associated genes regulated by human papillomavirus type 16 E6.
739 *Virology* **314**:196-205.
- 740 51. **Wong Y-F, Cheung T-H, Tsao GSW, Lo KWK, Yim S-F, Wang VW, Heung MMS,**
741 **Chan SCS, Chan LKY, Ho TWF, Wong KKY, Li C, Guo Y, Chung TKH, Smith DI.**
742 2006. Genome-wide gene expression profiling of cervical cancer in Hong Kong
743 women by oligonucleotide microarray. *Int J Cancer* **118**:2461-2469.
- 744 52. **Woodworth CD, S. C, S. S, Hamacher L, Chow LT, T.R. B, DiPaolo JA.** 1992.
745 Recombinant retroviruses encoding human papilloamvirus type 18 E6 and E7 genes
746 stimulate proliferation and delay differentiation of human keratinocytes early after
747 infection. *Oncogene* **7**:8.
- 748 53. **Richards KH, Wasson CW, Watherston O, Doble R, Eric Blair G, Wittmann M,**
749 **Macdonald A.** 2015. The human papillomavirus (HPV) E7 protein antagonises an
750 Imiquimod-induced inflammatory pathway in primary human keratinocytes. *Sci Rep*
751 **5**:12922.
- 752 54. **Rincon-Orozco B, Halec G, Rosenberger S, Muschik D, Nindl I, Bachmann A,**
753 **Ritter TM, Dondog B, Ly R, Bosch FX, Zawatzky R, Rösl F.** 2009. Epigenetic
754 silencing of interferon- κ in human papillomavirus type 16–positive cells. *Cancer Res*
755 **69**:8718-8725.
- 756 55. **Muto V, Stellacci E, Lamberti AG, Perrotti E, Carrabba A, Matera G, Sgarbanti**
757 **M, Battistini A, Liberto MC, Focà A.** 2011. Human papillomavirus type 16 E5
758 protein induces expression of beta interferon through interferon regulatory factor 1 in
759 human keratinocytes. *J Virol* **85**:5070-5080.
- 760 56. **Terenzi F, Saikia P, Sen GC.** 2008. Interferon-inducible protein, P56, inhibits HPV
761 DNA replication by binding to the viral protein E1. *EMBO J* **27**:3311-3321.

- 762 57. **Saikia P, Fensterl V, Sen GC.** 2010. The inhibitory action of P56 on select functions
763 of E1 mediates interferon's effect on human papillomavirus DNA replication. *J Virol*
764 **84**:13036-13039.
- 765 58. **Warren CJ, Xu T, Guo K, Griffin LM, Westrich JA, Lee D, Lambert PF, Santiago**
766 **ML, Pyeon D.** 2015. APOBEC3A functions as a restriction factor of human
767 papillomavirus. *J Virol* **89**:688-702.
- 768 59. **Meuris F, Carthagena L, Jaracz-Ros A, Gaudin F, Cutolo P, Deback C, Xue Y,**
769 **Thierry F, Doorbar J, Bachelerie F.** 2016. The CXCL12/CXCR4 signaling pathway:
770 a new susceptibility factor in human papillomavirus pathogenesis. *PLoS Pathog*
771 **12**:e1006039.
- 772 60. **Sivaprasad U, Kinker KG, Ericksen MB, Lindsey M, Gibson AM, Bass SA,**
773 **Hershey NS, Deng J, Medvedovic M, Khurana Hershey GK.** 2015. SERPINB3/B4
774 contributes to early inflammation and barrier dysfunction in an experimental murine
775 model of atopic dermatitis. *J Invest Dermatol* **135**:160-169.
- 776 61. **Hong S, Mehta KP, Laimins LA.** 2011. Suppression of STAT-1 Expression by
777 human papillomaviruses is necessary for differentiation-dependent genome
778 amplification and plasmid maintenance. *J Virol* **85**:9486-9494.
- 779 62. **Smith SP, Scarpini CG, Groves IJ, Odle RI, Coleman N.** 2016. Identification of
780 host transcriptional networks showing concentration-dependent regulation by HPV16
781 E6 and E7 proteins in basal cervical squamous epithelial cells. *Sci Rep* **6**:29832.
- 782 63. **Gray E, Pett M, Ward D, Winder DM, Stanley MA, Roberts I, Scarpini CG,**
783 **Coleman N.** 2010. *In vitro* progression of human papillomavirus 16 episome-
784 associated cervical neoplasia displays fundamental similarities to integrant-
785 associated carcinogenesis. *Cancer Res* **70**:4081-4091.
- 786 64. **Smith JHF, Patnick J.** 2013. Achievable standards, benchmarks for reporting and
787 criteria for conducting cervical cytopathology. (2nd Edition). Sheffield. NHS Cancers
788 Screening Programmes – available from [www.cancerscreening.nhs.uk/cervical](http://www.cancerscreening.nhs.uk/cervical/publications/nhscsp01.html)
789 [/publications/nhscsp01.html](http://www.cancerscreening.nhs.uk/cervical/publications/nhscsp01.html)

- 790 65. **Luesley, D. Leeson, S.** 2010. Colposcopy and Programme Management. NHS
791 Cancer Screening Programmes. (2nd Edition) Sheffield. NHS Cancers Screening
792 Programmes – available from [www.cancerscreening.nhs.uk/cervical/](http://www.cancerscreening.nhs.uk/cervical/publications/nhscsp20.html)
793 [publications/nhscsp20.html](http://www.cancerscreening.nhs.uk/cervical/publications/nhscsp20.html)
- 794 66. **Hirschowitz L.** 2012. Histopathology reporting in cervical screening-an integrated
795 approach. (2nd Edition) Sheffield. NHS Cancers Screening Programmes – available
796 from <http://www.cancerscreening.nhs.uk/cervical/publications/cc-04.html>
- 797 67. **Arbyn M, Ronco G, Anttila A, Meijer CJLM, Poljak M, Ogilvie G, Koliopoulos G,**
798 **Naucier P, Sankaranarayanan R, Peto J.** 2012. Evidence regarding human
799 papillomavirus testing in secondary prevention of cervical cancer. *Vaccine* **30**,
800 **Supplement 5:F88-F99.**
- 801 68. **Anders S, Huber W.** 2010. Differential expression analysis for sequence count data.
802 *Genome Biol***11**:1-12.
- 803 69. **The Gene Ontology C, Ashburner M, Ball CA, Blake JA, Botstein D, Butler H,**
804 **Cherry JM, Davis AP, Dolinski K, Dwight SS, Eppig JT, Harris MA, Hill DP, Issel-**
805 **Tarver L, Kasarskis A, Lewis S, Matese JC, Richardson JE, Ringwald M, Rubin**
806 **GM, Sherlock G.** 2000. Gene Ontology: tool for the unification of biology. *Nat Genet*
807 **25**:25-29.
- 808 70. **Ogata H, Goto S, Sato K, Fujibuchi W, Bono H, Kanehisa M.** 1999. KEGG: Kyoto
809 Encyclopedia of Genes and Genomes. *Nucleic Acids Res* **27**:29-34.
- 810 71. **Bindea G, Mlecnik B, Hackl H, Charoentong P, Tosolini M, Kirilovsky A,**
811 **Fridman W-H, Pagès F, Trajanoski Z, Galon J.** 2009. ClueGO: a Cytoscape plug-in
812 to decipher functionally grouped gene ontology and pathway annotation networks.
813 *Bioinformatics* **25**:1091-1093.
- 814
- 815

816 **Figure Legends**

817 **Figure 1. Characterisation of the HPV16 life cycle in NIKS16 and W12 cells.** A.

818 Expression levels of keratinocyte protein differentiation markers and viral L1 protein in
819 undifferentiated (U = monolayer culture for 5 days) and differentiated (D = monolayer culture
820 for 13 days) W12 and NIKS16 cells. GAPDH is shown as a loading control. B. Expression
821 levels of viral E2 and E4 proteins at 8 (mid differentiation phase) and 13 (differentiated) days
822 of a time course of NIKS16 differentiation in monolayer culture. C. Time course of involucrin
823 protein expression over a 13 day differentiation period (monolayer cells are mostly
824 undifferentiated after 5 days culture and fully differentiated after 13 days of culture) for NIKS
825 and NIKS16 cells. involucrin. D. Absolute quantification by qPCR of L1 gene copies,
826 as a measure of viral genomes, in differentiated W12 and NIKS16 cells. E. Viral late mRNA
827 levels quantified by detecting L1-containing mRNAs by qRT-PCR in undifferentiated and
828 differentiated W12 and NIKS16 cells. Invol, involucrin. K10, Keratin 10.

829 **Figure 2. HPV16 infection induces massive changes in the keratinocyte transcriptome.**

830 A. mRNA numbers expressed versus the level of expression of each individual mRNA in
831 undifferentiated (U) versus differentiated (D) NIKS (HPV-negative) cells. B. mRNA numbers
832 expressed versus the level of expression of each individual mRNA in undifferentiated (U)
833 versus differentiated (D) NIKS16 (HPV-positive) cells. C. Venn diagram showing the
834 percentage identity between upregulated genes of NIKS and NIKS16 cells compared to
835 NIKS and W12 cells. D. Venn diagram showing the percentage identity between
836 downregulated genes of NIKS and NIKS16 cells compared to NIKS and W12 cells. Identity
837 was determined using the GFOLD tool to calculate the differential fold changes of the two
838 comparisons.

839

840 **Figure 3. Keratinocyte differentiation and epithelial barrier function is altered by HPV**

841 **infection.** Significant changes in expression ($>\log_2=1.8$; 3.5-fold) of proteins involved in

842 keratinocyte differentiation and epithelial barrier function comparing HPV16-infected,
843 differentiated NIKS keratinocytes to uninfected, differentiated NIKS keratinocytes. These are
844 the mean values from three separate RNASeq experiments A. Markers of differentiation
845 (filaggrin, loricrin, involucrin and transglutaminase (TGM1)). B. Keratins (K). C.
846 Desmosomal proteins, desmogleins (DSG) 1 and 4 and desmocoilin (DSC). D. Gap
847 junction proteins, connexins (Cx) 26, 30.2 and 32. E. Claudins. F. Cadherins. G. small
848 proline rich proteins (SPRRs).

849

850 **Figure 4. ClueGO analysis of significantly up-and down-regulated genes in HPV16-**
851 **infected, differentiated NIKS keratinocytes compared to uninfected, differentiated**
852 **NIKS keratinocytes.** We used CluePedia, which extends ClueGO (71) functionality down to
853 genes, and visualizes the statistical dependencies (correlation) for markers of interest from
854 the experimental data. A. Gene ontology (GO) pathway terms specific for up-regulated
855 genes. B. GO pathway terms specific for down-regulated genes. The bars represent the
856 numbers of genes associated with the term on the left hand side. The percentage of altered
857 genes is shown above each bar. Red asterisks refer to significance. C. Functionally grouped
858 network for up-regulated genes. D. Functionally grouped networks for down-regulated
859 genes. Only the label of the most significant term per group is shown. The size of the nodes
860 reflects the degree of enrichment of the terms. The network was automatically laid out using
861 the organic layout algorithm in Cytoscape. Only functional groups represented by their most
862 significant term were visualized in the network. $P_{adj} < 0.05$ changes were analysed.

863 **Figure 5. Interactome of negatively and positively changed genes comparing**
864 **differentiated NIKS with differentiated NIKS16 cells.** Interactome of genes linked
865 through statistical correlation of A. up-regulated and B. down-regulated genes from the
866 experimental data (p -value < 0.05). Grey lettering, and diamonds indicates genes identified in
867 the RNASeq data set. Black lettering indicates linked genes. Nodes for genes identified

868 in the data set are indicated by black box outlines. Dots/lines surrounding nodes indicate the
869 numbers of linked pathways. The pathways analysis was produced using Cluepedia
870 (<http://apps.cytoscape.org/apps/cluepedia>).

871

872 **Figure 6. Western blot analysis of proteins levels encoded by selected, significantly**
873 **altered mRNAs (Table 2).** Protein extracts were prepared from undifferentiated and
874 differentiated HPV-negative NIKS and HPV16-positive NIKS16 and W12 cell populations.
875 Much greater levels of involucrin (invol) were detected in the differentiated, compared to the
876 undifferentiated cell populations indicating differentiation was achieved. GAPDH was used a
877 protein loading control. A. Protein levels corresponding to significantly up-regulated mRNAs.
878 B. Protein levels corresponding to significantly down-regulated mRNAs. U, undifferentiated.
879 D, differentiated.

880 **Figure 7. Expression levels of selected, significantly altered mRNAs in different**
881 **grades of HPV-associated pre-neoplastic cervical disease.** mRNA expression levels
882 were calculated from qPCR data using GAPDH and beta-actin as the internal controls and
883 expressed relative to levels in a single sample of differentiated, HPV16-positive W12 cell
884 RNA that was included in every PCR run. NDD, no detectable disease/borderline, all HPV-
885 negative. Low grade, cervical intraepithelial neoplasia 1 (CIN1), all HPV-positive. High grade
886 disease, cervical intraepithelial neoplasia 1 (CIN3), all HPV-positive.

Figure 1 KlymenkoNGS

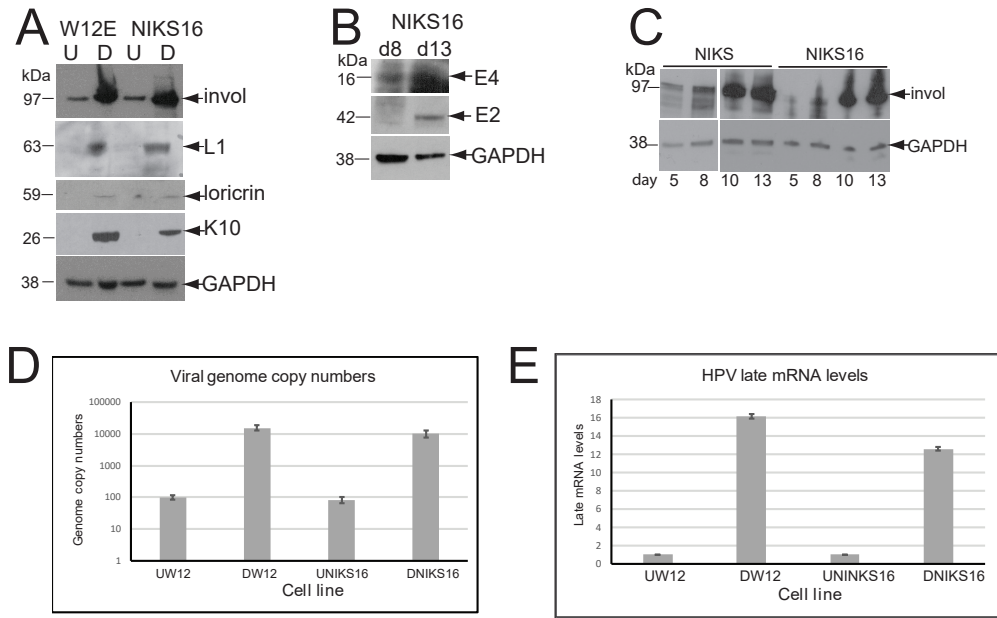


Figure 1 KlymenkoNGS

Figure 2 KlymenkoNGS

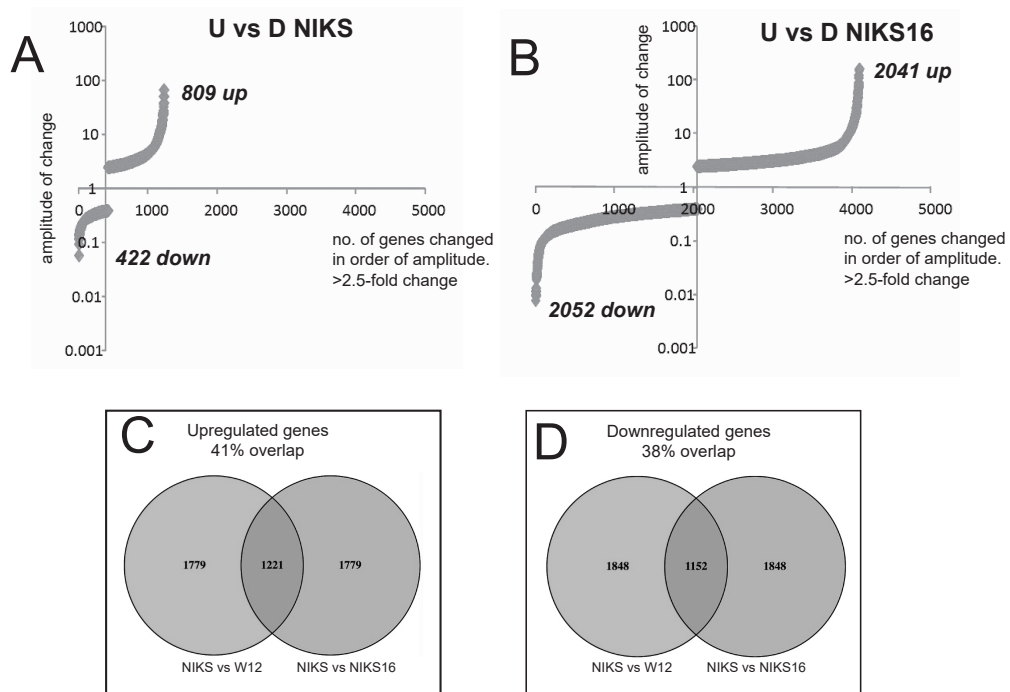


Figure 3 Klymenko et al.

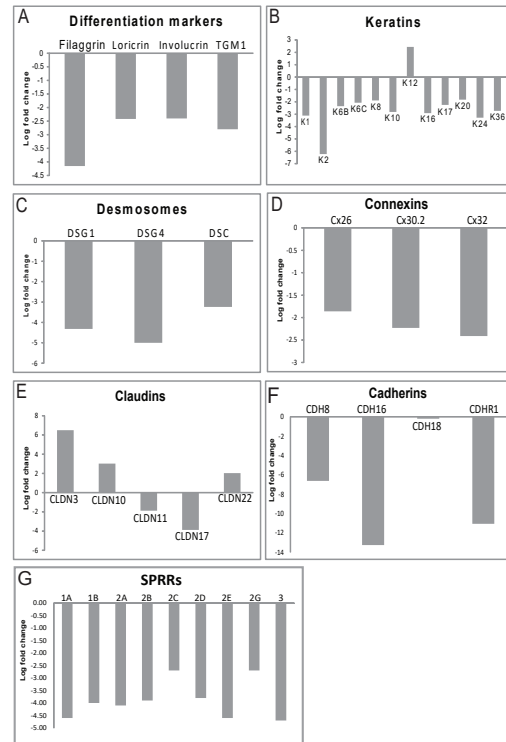


Figure 3 Klymenko et al.

Figure 4 Klymenko et al.

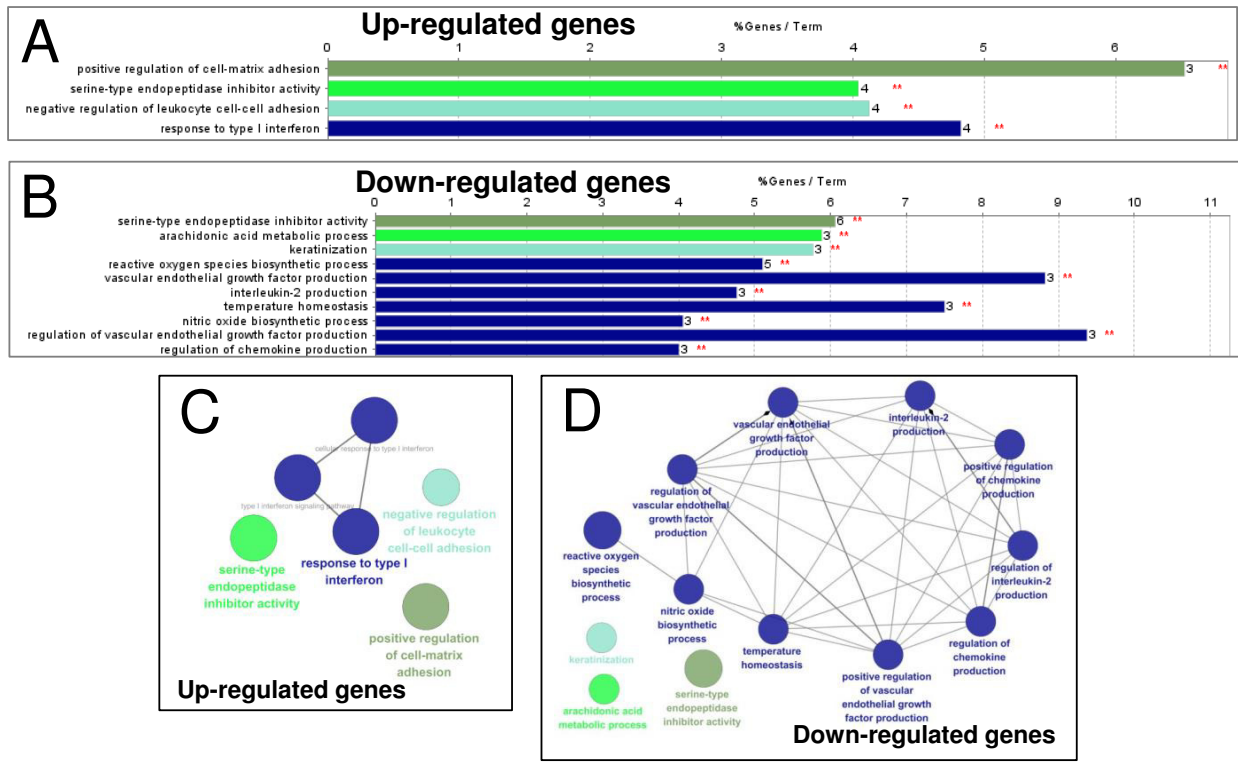


Figure 6 Klymenko et al.

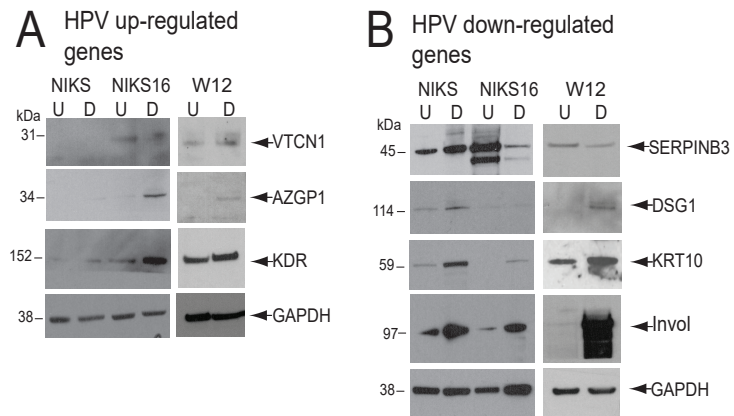


Figure 6 Klymenko et al.

Klymenko et al. Figure 7

